International Journal of Heat and Mass Transfer 52 (2009) 1295–1303

Contents lists available at ScienceDirect

International Journal of Heat and Mass Transfer

journal homepage: www.elsevier.com/locate/ijhmt

Physical mechanisms of heat transfer during single bubble nucleate boiling of FC-72 under saturation conditions-II: Theoretical analysis

Saeed Moghaddam [a,*], Ken Kiger [b]

[a] Department of Mechanical Science and Engineering, University of Illinois at Urbana-Champaign, 1206 West Green Street, Urbana, IL 61801, USA
[b] Department of Mechanical Engineering, University of Maryland, 2181 Glenn L. Martin Hall, College Park, MD 20742, USA

ARTICLE INFO

Article history:
Received 2 April 2008
Received in revised form 22 August 2008
Available online 13 November 2008

Keywords:
Heat transfer
Boiling
Microlayer evaporation
Transient conduction
Microconvection

ABSTRACT

This paper is the second part of a two-part study concerning the dynamics of heat transfer during the nucleation process of FC-72 liquid. The experimental findings on the nature of different heat transfer mechanisms involved in the nucleation process were discussed in part I. In this paper, the experimental results are compared with the existing boiling models. The boiling models based on dominance of a single mechanism of heat transfer did not match the experimental results. However, the Rohsenow model was found to closely predict the heat transfer through the microconvection mechanism that is primarily active outside the bubble/surface contact area. An existing transient conduction model was modified to predict the surface heat transfer during the rewetting process (i.e. transient conduction mechanism). This model takes into account the gradual rewetting of the surface during the transient conduction process rather than a simple sudden surface coverage assumption commonly used in the boiling literature. The initial superheat energy of the microlayer (i.e. microlayer sensible energy) was accurately calculated and found to significantly contribute in microlayer evaporation. This even exceeded the direct wall heat transfer to microlayer at high surface superheat temperatures. A composite model was introduced that closely matches our experimental results. It incorporates models for three mechanisms of heat transfer including microlayer evaporation, transient conduction, microconvection, as well as their influence area and activation time. The significance of this development is that, for the first time, all submodels of the composite correlation were independently verified using experimental results.

Published by Elsevier Ltd.

1. Introduction

Over the past 50 years, several mechanistic models (i.e. based on the physics of a process) have been developed to predict the surface heat transfer during the nucleate boiling process. These models have been commonly used to predict the surface heat transfer on large boiling surfaces which simultaneously generate numerous bubbles. On a large boiling surface, interactions between the bubbles would likely trigger a more complex regime of heat transfer than in the case of a single bubble boiling (conditions discussed in part I of this study). Although the existing mechanistic boiling models were often applied to such regimes, they do not have built-in mechanisms to model the heat transfer processes resulting from interactions between the bubbles. In fact, quite to the contrary, they have frequently been developed solely based on assumptions concerning the heat transfer processes involved in single bubble boiling. In addition, empirical coefficients were often used to accommodate for differences between the models and the experimental results, but without any clear *a priori* indication as to the cause of the discrepancy.

In this study, we use the experimental results presented in part I to examine the fundamental assumptions of several representative mechanistic models available in the boiling literature and discuss the strength and weaknesses of the models. One can readily appreciate that the most accurate way to test the underlying physics of these models is to compare them with experimental single bubble boiling results (i.e. eliminate the effect of multiple bubbles) in which all the parameters used to construct the models are accurately measured. Due to the difficult nature of the experiments required in such a task, historically this has rarely been done. Rather, the models are usually tested through comparison to some bulk measured value, such as average heat flux, leaving the soundness of the original physical assumptions open to speculation. To set the stage for this analysis/comparison, a survey of the most popular boiling models is provided in the following. The existing models have been divided into three different categories, each with a fundamentally different modeling approach.

The first category of models have attempted to simplify the essence of the boiling heat transfer process to mechanisms normally attributed to steady single phase heat transfer. In these models, the role of phase-change processes is relegated to the role of secondary parameters, which indirectly influence the resulting heat transfer. Jakob and Linke [1] were probably the first to suggest that the

* Corresponding author. Tel.: +1 217 244 5136; fax: +1 217 244 6534.
E-mail address: saeedmog@uiuc.edu (S. Moghaddam).

0017-9310/$ - see front matter Published by Elsevier Ltd.
doi:10.1016/j.ijheatmasstransfer.2008.08.024

Nomenclature

A_c	contact area [m^2]
A_m	microlayer area [m^2]
A_T	total heat transfer surface area [m^2]
C	specific heat [J/kg K]
C_1	coefficient in Eq. (3)
C_d	coefficient in Eq. (4)
C_q	coefficient in Eq. (6)
C_{sf}	coefficient in Eq. (2)
D_b	bubble diameter [m]
D_c	diameter of contact area [m]
f	bubble departure frequency [1/s]
Ja	Jacob number
h_{lv}	heat of vaporization [J/kg]
k	thermal conductivity [W/m K]
K	coefficient in Eq. (23)
m	mass [kg]
n	nucleation site density [$1/m^2$]
N	number of nucleation sites
Nu	Nusselt number
Nu_{NC}	natural convection Nusselt number
Nu_{Roh}	Rohsenow Nusselt number (Eq. (7))
Pr	Prandtel number
$q''(t)$	heat flux [W/m^2]
q''	average heat flux [W/m^2]
q''_{ME}	microlayer evaporation heat flux [W/m^2]
q''_{MC}	microconvection heat flux [W/m^2]
q''_{NC}	natural convection heat flux [W/m^2]
q''_{TC}	transient conduction heat flux [W/m^2]
Q_{ME}	microlayer evaporation energy [J]
Q_{TC}	energy transferred through transient conduction [J]
r_1	larger radius of a sensor [m]
r_2	smaller radius of a sensor [m]
r_c	radius of contact area [m]
r', r''	radial position [m]
Ra	Rayleigh number
R_b	bubble radius [m]
Re	Reynolds number
t	time [s]
t',t''	time [s]
t_0	initial bubble formation time [s]
t_g	bubble growth time period [s]
t_m	microlayer evaporation time [s]
t_r	duration of the surface rewetting event [s]
$t_{ME,i}$	beginning of microlayer evaporation [s]
$t_{ME,e}$	end of microlayer evaporation [s]
t_w	bubble waiting time [s]
$\overline{T}_m$	average microlayer temperature [°C]
T_s	surface temperature [°C]
T_{sat}	liquid saturation temperature [°C]
U_b	bubble/liquid interface velocity during bubble growth [m/s]
v	contact line velocity [m/s]
V_{δ_0}	microlayer initial volume [m^3]

Greek symbols

ΔT	surface superheat temperature [°C]
ΔT_{TC}	surface and rewetting liquid temperature difference [°C]
Δx	thickness of BCB film [m]
ρ	density [kg/m^3]
δ_0	microlayer initial thickness [m]
$\bar{\delta}_0$	average microlayer thickness, $V_{\delta_0}/\phi\pi R_b^2$ [m]
α	thermal diffusivity [m^2/s]
β	expansion coefficient [K^{-1}]
σ	surface tension [N/m]
θ	contact angle [degree]
ϕ	ratio of contact area and bubble projected area, $(D_c/D_b)^2$
μ	dynamic viscosity [N s/m^2]
ν	kinematic viscosity [m^2/s]

Subscripts

b	bubble
l	liquid
v	vapor

primary mechanism of heat transfer from a boiling surface is sensible heat transfer to the liquid, and therefore should follow a convective scaling. The most popular model developed on this basis is that of Rohsenow [2], in which he adapted a single-phase convective heat transfer correlation (i.e. $Nu = CRe^mPr^n$), using the bubble diameter and vapor superficial velocity as the relevant characteristic length and velocity scale to determine the *Re* number. In a similar analogy, Tien [3] noted that the wake generated behind a rising bubble resembles the velocity distribution of a reversed axisymmetric stagnation flow. He then used the heat transfer correlation for a stagnation flow [4] to develop a correlation for the boiling heat transfer coefficient. In another effort, Zuber [5] assumed a similarity between boiling and turbulent natural convection flow to develop a correlation based on a single phase heat transfer analogy.

In the second category of models, researchers strived to provide a more explicit connection between the transient bubble dynamics and the resulting convective environment. Along these lines, Forster and Greif [6] postulated that bubbles act as micropumps that transport superheated liquid into the bulk as they grow and depart from the surface. The total heat transferred through subsequent pumping action was calculated using the volume of the bubble and its frequency. They used the difference between the wall and bulk liquid temperatures to define the energy transported in the pumping action. Mikic and Rohsenow [7] postulated that heat transfer during boiling mainly occurs in a transient conduction heat transfer process. They assumed that a departing bubble pumps away the hot liquid adjacent to the surface from an area twice the bubble diameter. They approximated the transient heat transfer into the near-wall entrained liquid using the transient conduction solution through a semi-infinite body (the liquid), while simultaneously excluding heat transfer from areas outside the bubble influence region. Haider and Webb [8] extended the Mikic and Rohsenow [7] model by including the effect of another mechanism of heat transfer that they called transient convection. This mechanism of heat transfer was suggested to arise as a result of convection in the wake of the departing bubbles. In order to evaluate their model using the existing data on large surfaces, Haider and Webb [8] used an existing model for nucleation site density. Then, they tried to fit their model to experimental data by changing the weight factors considered for each mechanism of heat transfer. Their analysis suggested that transient convection is the dominant heat transfer mode.

The third group of models assumed that different mechanisms of heat transfer are active during the boiling process. These models [9–15] accounted for latent heat transfer in addition to the sensible heat transfer to the liquid. For example, Judd and Hwang [12] and more recently Dhir [15] envisaged that by combining the contributions of microlayer evaporation, transient conduction, and natural convection one can determine a more comprehensive boiling heat transfer correlation. Dhir [15] further elaborated that for this

correlation to be verified as a predictive tool, one needs to have closure models for several parameters: bubble diameter, bubble departure frequency, diameter of the area influenced by the bubble, the average heat transfer coefficients for natural convection and microlayer evaporation. Although models exist in the literature for some of these parameters, there is no consensus on how well they function, or even over what general region of parametric space they should be used.

The experimental results presented in part I of this study suggested that all mechanisms of heat transfer can have a significant contribution in total surface heat flux, even when focusing on a restricted region of the parametric space (highly wetting fluid on a conductive substrate at saturation conditions). Therefore, none of the models that assume dominance of a single mode of heat transfer represents the actual physics of the heat transfer process. So, it is clear that a composite model should better fit our experimental results. In the following section, we first evaluate the ability of the single mode models to predict their corresponding mechanism of heat transfer measured in our tests and then discuss the composite models. Furthermore, using the high-resolution data from part I concerning the details of the heat transfer mechanisms (magnitude, area of influence, time period of activation, etc.), the existing models will be fine tuned and eventually combined into a single composite model.

2. Experimental *Nu* number

The experimental results reported in a companion paper [16] are used to provide a detailed data set to test the models. Tests were conducted over a range of superheat values in which the time- and space-resolved surface temperature, heat flux, and bubble size were determined. Using the experimental bubble departure diameter as the characteristic length, the time- and space-averaged surface temperature, and the average surface heat flux, the surface *Nu* number was determined as follows

$$Nu = \frac{hD_b}{k_l} = \frac{q''D_b}{(\Delta T)k_l} \tag{1}$$

Fig. 1 shows the experimental values of the average surface heat flux (q'') and bubble diameter and Fig. 2 shows the calculated *Nu* number. Thermophysical properties of the FC-72 liquid are provided in Table 1. As can be seen in Fig. 2, the *Nu* number increases with the surface temperature.

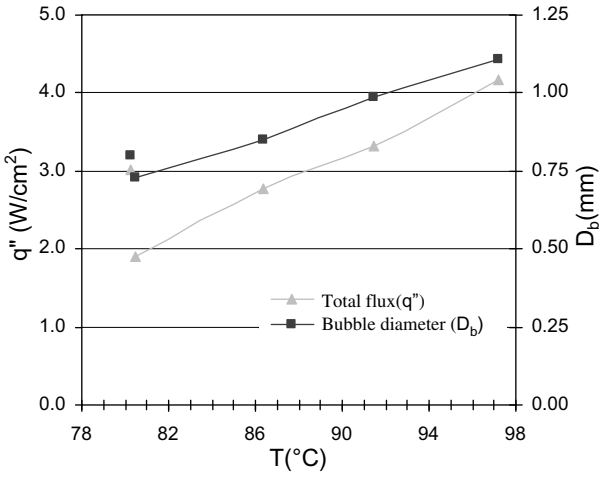

Fig. 1. Total surface heat flux and bubble departure diameter at different tests.

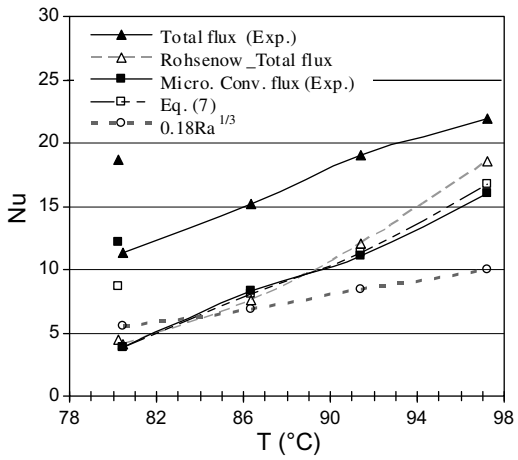

Fig. 2. Comparison of the experimental Nusselt number corresponding to total surface heat flux and microconvection heat flux with theory.

Table 1
Thermophysical properties of FC-72 liquid at saturation conditions [27]

Parameter	Values
ρ_l	1619.7 [kg/m^3]
ρ_v	13.4 [kg/m^3]
k_l	0.052 [W/m K]
α_l	2.93×10^{-8} [m^2/s]
μ_l	4.54×10^{-4} [N s/m^2]
C_l	1098.4 [J/kg K]
h_{fg}	84510.9 [J/kg]
Pr_l	9.56
σ	8.27×10^{-3} [N/m]

3. Convection models

3.1. Rohsenow [2] model

Rohsenow [2] suggested the following equation for nucleate boiling heat transfer (note that the exponent of 1.7 for *Pr* is applicable for any liquid except water [2]):

$$\frac{C_l(\Delta T)}{h_{lv}} = C_{sf}\left(\frac{q''}{\mu_l h_{lv}}\sqrt{\frac{\sigma}{g(\rho_l-\rho)}}\right)^{0.33} Pr_l^{1.7} \tag{2}$$

The value of C_{sf} depends on the combination of the surface and liquid properties that should be determined experimentally. For different combinations of liquid and surface material, Rohsenow [2] suggested a range of 0.0027–0.0154 for C_{sf}. A value of 0.013 was recommended for C_{sf} as a first approximation when no experimental data is available. The theoretical heat flux was calculated using Eq. (2) and C_{sf} = 0.013. The corresponding *Nu* was then calculated using Eq. (1) and reported in Fig. 2. Overall, the Rohsenow [2] model underpredicted the experimental results, especially at low surface temperature. Its prediction is only 36.3% of the experimental value at low surface temperature (80.5 °C) and 84.3% of the experimental value at high surface temperature (97.2 °C). The Rohsenow [2] model particularly failed to distinguish any difference between the test results with and without waiting time (tests No. 5 and No. 1 in [16]) at low surface temperature. This is due to the fact that heat flux in Eq. (2) is only a function of ΔT and liquid properties.

Since the fundamental assumption of the Rohsenow [2] model is bubble induced convection and we have seen such an effect (i.e. microconvection observed outside the contact area), the experimental *Nu* number has been calculated using the microconvection heat flux values (cf. Fig. 2). Overall, the results were close

to the Rohsenow [2] *Nu* number, except for test case with waiting time due to the reason mentioned above. Failure of the Rohsenow [2] model to distinguish any difference in heat flux resulted from differences in nucleation dynamics at a similar surface temperature is certainly a fundamental issue. Since the Rohsenow [2] model is developed based on convection induced by bubbles, one might suggests that it should take into account differences in bubbling dynamics. In order to explore this issue, we started with the original convection equation used by Rohsenow [2]

$$Nu = C_1 Re^m Pr_l^n \tag{3}$$

and reverted it to the original elements used in derivation of Eq. (2). Rohsenow [2] used the following equations for the bubble diameter and *Re* number

$$D_b = C_d\theta\left[\frac{2\sigma}{g(\rho_l-\rho_v)}\right]^{0.5} \tag{4}$$

$$Re_b = \frac{G_b D_b}{\mu_l} \tag{5}$$

where $C_d\theta$ is a function of liquid and surface properties and G_b is related to the surface heat flux through the following equation.

$$q'' = C_q h_{lv} G_b = C_q h_{lv}\left(\rho_v \frac{\pi}{6} D_b^3 fn\right) \tag{6}$$

Using Eqs. (4)–(6) and (1) for the *Nu* number, Eq. (2) can be written as follow

$$Nu = \frac{C_q}{C_{sf}\left(\frac{C_q}{\sqrt{2}C_d\theta}\right)^{0.33}} Re_b^{0.67} Pr_l^{-0.7} \tag{7}$$

Using the experimental data for the bubble diameter and liquid properties, the coefficient $C_d\theta$ that represents the liquid and surface combination properties was determined. Since the area of interest for heat transfer calculation is D_b, the following equation for n was used to determine C_q using Eq. (6).

$$n = \frac{N}{A_T} = \frac{1}{\pi D_b^2/4} \tag{8}$$

Note that the values of factors C_d and C_q change at different test conditions. Eventually, using a value of 0.013 for C_{sf} and Eq. (5) for Re_b, *Nu* was determined using Eq. (7). Results are presented in Fig. 2.

Results suggested a close agreement between theory and experiment over the entire temperature range. The main highlight of this comparison is that the open form of Rohsenow [2] model (i.e. Eq. (7)) allowed differentiating between *Nu* numbers of two different nucleation (tests No. 5 and No. 1 [16]) regimes at a similar surface and liquid temperature. This was mainly due the difference in C_1 coefficient that was 33.6 for test No. 5 versus 15.9 for test No. 1. The difference in *Re* number between the two was small (1.4 and 1.3 for test No. 5 and 1, respectively).

Although the Rohsenow [2] model predicted the test results for microconvection heat transfer closely, this agreement does not corroborate Rohsenow's [2] idea as a basis for microconvection heat transfer. Obviously, using other values of C_{sf} determined for other surface/liquid combinations changes the results. It is not clear whether Rohsenow [2] had any other reason for recommending 0.013 as a starting point for modeling/prediction other than the fact that this coefficient corresponded to water (boiled on polished platinum) that has been a popular boiling liquid (especially during the 1950s in boiling water nuclear reactors and power plants).

3.2. Forster and Zuber [17] model

Forster and Zuber [17] followed the Rohsenow's analogy [2] for the mechanism of heat transfer, but modified the expression for the bubble radius and velocity ($R_b = Ja(\pi\alpha_l t)^{1/2}$ and $U_b = dR_b/dt$) to calculate $Re_b(=\frac{\rho_v U_b D_b}{\mu_l})$. Using these modified expressions, they arrived at the following equation for Re_b.

$$Re_b = \frac{\rho_l}{\mu_l}\left(\frac{\Delta T C_l \rho_l \sqrt{\pi\alpha_l}}{h_{lv}\rho_v}\right)^2 \tag{9}$$

and recommended the following correlation for *Nu* after fitting their model to experimental data.

$$Nu = 0.0015 Re_b^{0.62} Pr_l^{0.33} \tag{10}$$

Eq. (10) determines a *Nu* of 0.14–0.27 for the surface temperature range of 80.5–97.2 °C. The results are significantly lower than the experimental values as well as the predictions of the Rohsenow [2] model. It is interesting that even though Forster and Zuber [16] used a similar analogy to that of Rohsenow [2] their end result is quite different. Aside from the more obvious difference that is between the *Pr* exponent in the two correlations (0.33 in Forster and Zuber's versus −0.7 in Rohsenow's), the values of C_1 (see Eq. (3)) and Re_b are also significantly different. C_1 is 0.0015 in the Forster and Zuber's correlation and between 36.7 (at 80.5 °C) and 73.9 (at 97.4 °C) in the Rohsenow's correlation. Eq. (9) determines a Re_b of 461.5–1335.2 for low to high surface temperatures, respectively, versus the much smaller values of 1.3–2.01 determined from Eq. (5).

4. Transient conduction models

4.1. Mikic and Rohsenow [7] model

Mikic and Rohsenow [7] suggested that a departing bubble continuously pumps the hot liquid away from the surface and heat is transferred via transient conduction into the liquid that replaces the displaced fluid. They considered this mechanism to be the sole mechanism of heat transfer from the surface. They used the governing equation for heat transfer to a semi-infinite body [18] and derived the following equation for surface heat flux.

$$q'' = f\int_0^{\frac{1}{f}} \frac{k_l \Delta T}{\sqrt{\pi\alpha_l t}} dt = 2\frac{k_l \Delta T}{\sqrt{\pi\alpha_l}}\sqrt{f} \tag{11}$$

Eq. (11) can be written in *Nu* form as follows,

$$Nu = \frac{2}{\sqrt{\pi}}\left(\frac{f.D_b^2}{\alpha_l}\right)^{0.5} \tag{12}$$

Using Eq. (12) and the experimental values of bubble departure frequency (f) and diameter (D_b), *Nu* at different surface temperatures were calculated. The transient conduction model of Mikic and Rohsenow [7] predicted *Nu* values that were a few times greater than the experimental results. In order to find out whether the Mikic and Rohsenow [7] model matches the transient conduction part of the test results, *Nu* values were calculated using the average transient conduction heat flux at the contact area. As can be seen in Fig. 3, the results are still lower than the Mikic and Rohsenow [7] predictions. The main reason for this difference could be found by examining the experimental results presented in the first part of this study. The test results suggested that unlike what is assumed in the Mikic and Rohsenow [7] model (i.e. sudden coverage of the entire surface with bulk liquid), the process of surface rewetting is gradual. During this process, the contact line rewets the surface with a finite velocity. So, the overall surface heat transfer is small before a significant part of the surface is covered with liquid.

In order to better understand the physics of this process, heat transfer results of the individual sensors have been analyzed. Fig. 4 shows typical experimental data for the cumulative heat

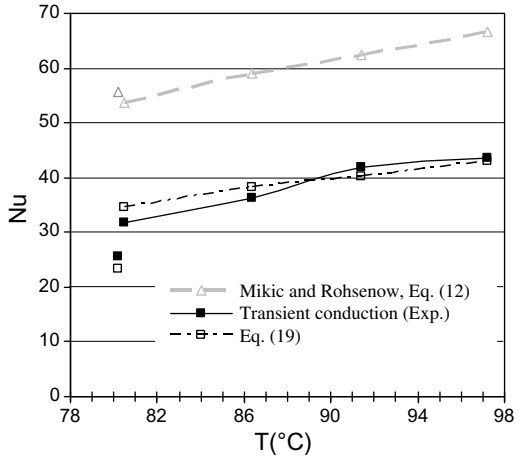

Fig. 3. Comparison of the Nusselt number corresponding to transient conduction heat flux with theory.

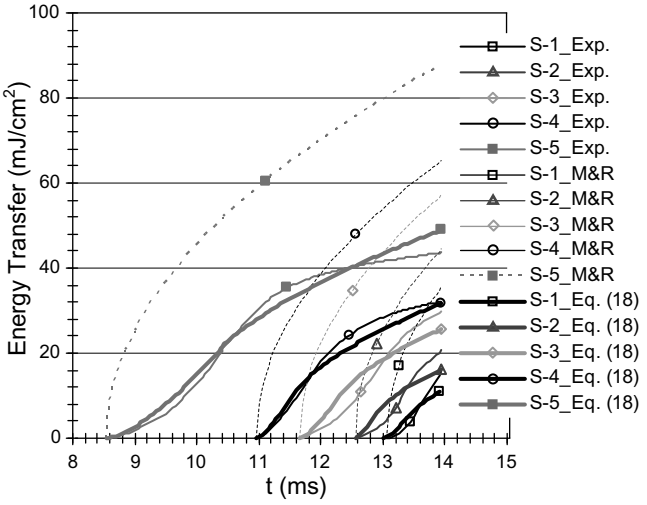

Fig. 4. Comparison between experimental and theoretical values of transient conduction heat transfer of different sensors (at surface temperature of 91.4 °C).

transfer of the individual sensors and their comparison with the Mikic and Rohsenow [7] model. Clearly, the model does not follow the experimental results. Demiray and Kim [19] modified the transient conduction model to account for the gradual surface coverage. They determined an expression for surface heat flux by integrating the governing equation for heat flux at an arbitrary point r' (cf. Fig. 5) when it is covered with the liquid front at t'.

$$q_{TC}(t) = \int_r^{r_1} \frac{k\Delta T_{TC}}{\sqrt{\pi\alpha}} \frac{2\pi r' dr'}{\sqrt{t-t'}} \tag{13}$$

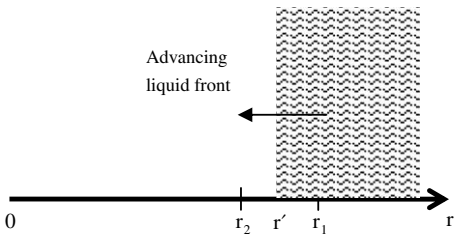

Fig. 5. Schematic of the advancing liquid front on the heat transfer surface.

After substituting t and t' with $t = (r_1 - r)/v$ and $t' = (r_1 - r')/v$ the following equation is determined.

$$q_{TC}(t) = \frac{2\pi k\Delta T_{TC}\sqrt{v}}{\sqrt{\pi\alpha}} \int_r^{r_1} \frac{r' dr'}{\sqrt{r'-r}} \tag{14}$$

$$q_{TC}(t) = \frac{4\pi k\Delta T_{TC}\sqrt{v}}{\sqrt{\pi\alpha}} \left(r_1 t^{1/2} - \frac{2}{3} v t^{3/2} \right) \tag{15}$$

Eq. (15) is only valid until the surface is completely rewetted by the liquid front. But, as can be seen in Fig. 4, heat transfer continues long after the liquid front passes over a sensor. So, an expression for heat flux should be developed after the contact line reaches r_2 at $t_r = (r_1 - r_2)/$. This was achieved by integrating the governing equation for heat flux at an arbitrary point r'' that has been in contact with liquid for $t - t'' = t - (r_1 - r'')/$.

$$q_{TC}(t) = \int_{r_2}^{r_1} \frac{k\Delta T_{TC}}{\sqrt{\pi\alpha}} \frac{2\pi r'' dr''}{\sqrt{t-t''}} \tag{16}$$

$$q_{TC}(t) = \frac{4\pi k\Delta T_{TC}\sqrt{v}}{\sqrt{\pi\alpha}} \Big((r_1 - vt)(t^{1/2} - (t-t_r)^{1/2}) + \frac{v}{3}\left(t^{3/2} - (t-t_r)^{3/2} \right) \Big) \tag{17}$$

Eqs. (15) should be used before and (17) after, respectively, complete surface coverage at t_r to determine surface heat flux on a gradually covered surface. Both equations can be integrated and combined to determine the cumulative surface heat transfer.

$$Q_{TC} = \begin{cases} \frac{8\pi k\Delta T_{TC} v}{3\sqrt{\pi\alpha}} \left(r_1 t^{3/2} - \frac{2}{5} v t^{5/2} \right) & \text{for } t < t_r \\ \frac{8\pi k\Delta T_{TC} v}{3\sqrt{\pi\alpha}} \left(r_1 t_r^{3/2} - \frac{2}{5} v t_r^{5/2} + r_1 (t^{3/2} - t_r^{3/2}) \right. & \text{for } t \geqslant t_r \\ \left. -(r_1 - vt_r)(t-t_r)^{3/2} - \frac{2v}{5}(t^{5/2} - t_r^{5/2}) + \frac{2v}{5}(t-t_r)^{5/2} \right) & \end{cases} \tag{18}$$

Fig. 4 compares the cumulative heat transfer results (divided by surface area of each sensor) determined using Eq. (18). Results show a relatively close match to experiment with $\Delta T_{TC} = 0.65\Delta T$. This agreement suggests that transient conduction heat transfer correlates well with the transient conduction theory when gradual surface coverage is taken into account. The results also suggest that the temperature difference between the rewetting liquid and surface is lower than the surface superheat temperature. The ratio of $\Delta T_{TC}/\Delta T$ was between 0.55 and 0.65 at different surface temperatures.

The second part of Eq. (18) is used (r_1 is substituted by r_c) to determine the equivalent average surface heat flux due to the transient conduction process:

$$q''_{TC} = \frac{Q_{TC}}{A_c t} = \frac{8k\Delta T_{TC} v}{3\sqrt{\pi\alpha} r_c^2 t} \left(r_c t_r^{3/2} - \frac{2}{5} v t_r^{5/2} + r_c (t^{3/2} - t_r^{3/2}) - (r_c - vt_r)(t-t_r)^{3/2} - \frac{2v}{5}(t^{5/2} - t_r^{5/2}) + \frac{2v}{5}(t-t_r)^{5/2} \right) \tag{19}$$

The contact area heat flux and the corresponding Nu were calculated using Eq. (19). An average value of $\Delta T_{TC}/\Delta T = 0.6$ was used and a close agreement (better than 9%) between the theory and the experiment was found. When the waiting time is almost zero (i.e. $t = t_r$), only the 1st and 2nd terms in Eq. (19) remain. As a result, a simplified expression for transient conduction heat transfer can be determined (note that $v = r_c/t_r$).

$$q''_{TC} = \frac{8}{5} \frac{k_l \Delta T_{TC}}{\sqrt{\pi\alpha_l t_r}} \tag{20}$$

Note that one can also replace t_r in Eq. (20) using its relation with bubble departure frequency (f). The experimental values of t_r and f are reported in Table 2. Comparison between the test results at different surface temperatures, when no waiting time

Table 2
Experimental data on transient conduction time, bubble departure frequency, and ratio of contact area to bubble diameters

Test No.	Surface temperature (°C)	t_r [ms]	f [1/s]	$1/t_r f$	D_c/D_b
1	80.5	4.75	125	1.7	0.52
2	86.4	4.7	112	1.9	0.55
3	91.4	5.9	92	1.8	0.53
4	97.2	6.65	83	1.8	0.54
5	80.2	3.7	112	2.4	0.58

exists between the bubbles suggest that $1/t_r f$ is relatively constant (=1.8). So, we replace t_r in Eq. (20) with $1/1.8f$ to determine

$$q''_{TC} = 2.15\frac{k_l \Delta T_{TC}}{\sqrt{\pi \alpha_l}}\sqrt{f} \tag{21}$$

and the following expression for Nu number

$$Nu = \frac{1.29}{\sqrt{\pi}}\left(\frac{f.D_b^2}{\alpha_l}\right)^{0.5} \tag{22}$$

Note that constant 1.29 only applies to the test results of this study and that q''_{TC} is not active during the entire bubbling cycle.

5. Composite models

5.1. Judd and Hwang [12] model

Judd and Hwang [12] envisaged that heat flux is comprised of three components: a microlayer evaporation component q''_{ME}, a transient conduction component q''_{TC}, and a natural convection component q''_{NC}. They assumed that the area of the surface involved in transient conduction heat transfer process is $K\pi R_b^2(N/A_T)$ and that of the natural convection process is $1 - K\pi R_b^2(N/A_T)$. Thus, they proposed the following correlation:

$$q'' = A_m(N/A_T)q''_{ME} + K\pi R_b^2(N/A_T)q''_{TC} + (1 - K\pi R_b^2(N/A_T))q''_{NC} \tag{23}$$

It was assumed that q''_{ME} is the average heat flux for evaporation of the entire microlayer volume. The Mikic and Rohsenow [7] model was used to calculate the transient conduction component. They used $Nu_{NC} = 0.18Ra_{D_b}^{1/3}$ to determine the natural convection heat flux. Their final correlation is as follow

$$q'' = \rho_l h_{lv} n f V_{\delta_0} + 2\frac{k_l}{\sqrt{\pi\alpha_l}}\sqrt{f}(K\pi R_b^2 n)\Delta T + 0.18k_l\left(\frac{g\beta_l}{\nu_l\alpha_l}\right)^{1/3} \times (1 - K\pi R_b^2 n)\Delta T^{4/3} \tag{24}$$

Judd and Hwang [12] used Voutsinos and Judd [20] experimental results (on dichloromethane) for the initial microlayer thickness (1–6 μm depending on the surface heat flux) to calculate the total microlayer volume. Also, they determined the nucleation site density ($n = N/A_T$) experimentally.

To test their model against experimental data, Judd and Hwang [12] substituted $K = 4$ in Eq. (24). The value of $K = 4$ used by Judd and Hwang [12] was inspired by the Mikic and Rohsenow [7] hypothesis that suggested a transient conduction influence area of twice the bubble diameter (i.e. four times the bubble projected area). The results, however, was significantly greater than the experimental data. Judd and Hwang [12] found the best fit to their experimental data using $K = 1.8$.

The first term in Eq. (24) requires calculation of the microlayer thickness. In addition, it suggests that the microlayer acquires its entire evaporation energy directly from the wall. Using the experimental data presented in part I of this study, the initial thickness of the microlayer as well as the ratio between its evaporation energy and the energy directly transferred to the microlayer from the wall can be calculated. The details are provided in the following section.

5.1.1. Microlayer thickness and its evaporation energy

The initial microlayer thickness can be calculated using the total energy required for its evaporation (i.e. latent heat of vaporization). The microlayer evaporation energy can be broken into two parts: (1) direct heat transfer from the heated wall ($\int_{t_{ME,i}}^{t_{ME,e}} q''_{ME} A dt$) during the microlayer evaporation and (2) the initial sensible energy of the microlayer ($mC_l(\overline{T}_m - T_{sat})$). The sum of these two components is equal to the microlayer evaporation energy (mh_{lv}). Therefore, the microlayer thickness can be determined [21] using the following equation.

$$\delta_0 = \int_{t_{ME,i}}^{t_{ME,e}} q''_{ME} dt/(\rho_l h_{lv} - \rho_l C_l \Delta\overline{T}_m) \tag{25}$$

Before one could use Eq. (25) to calculate the initial microlayer thickness, the initial average superheat temperature of the microlayer ($\Delta\overline{T}_m$) should be determined. Since the surface temperature and heat flux at the time of microlayer formation are known, the initial temperature profile in the vicinity of the wall can be directly calculated. Fig. 6 shows a schematic of the liquid temperature profile during the transient conduction heat transfer process. Knowing the surface heat flux, the slope of the temperature profile at the liquid and surface interface, $dT/dy = q''/k_l$, can be determined. Since the microlayer is only a few microns thick, the temperature profile within the microlayer can reasonably be approximated as linear. Furthermore, since the temperature of the bottom of the microlayer film is equal to the wall temperature, and the temperature gradient within the liquid is determined, the average temperature of the microlayer and thereby $\Delta\overline{T}_m$ can be calculated. Using Eq. (25), the initial thickness of the microlayer on each sensor was determined. Results are presented in Fig. 7a. Also, Fig. 7b shows the variation of the initial contact-area average microlayer thickness for the different test conditions. The total microlayer evaporation energy can then be determined using the following expression.

$$Q_{ME} = \rho_l V_{\delta_0} h_{lv} \tag{26}$$

The ratio of the microlayer evaporation energy and the energy directly transferred to the microlayer from the wall, as can be seen in Fig. 8, suggests that using only the initial microlayer thickness to calculate the wall heat transfer would lead to a significant overestimation (about 40% to 120% from low to high surface temperature) of the total surface heat flux via microlayer evaporation mechanism.

The second term of the Judd and Hwang [12] model represents heat transfer through transient conduction process. This term also significantly overpredicts the transient component of the surface heat flux for the following three reasons:

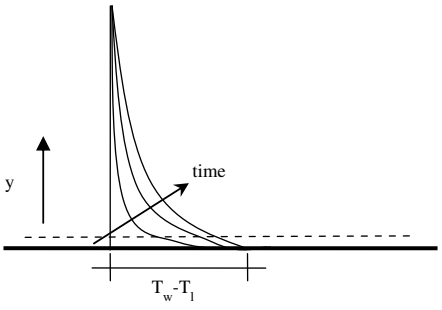

Fig. 6. Schematic of temperature profile within the liquid before the microlayer formation.

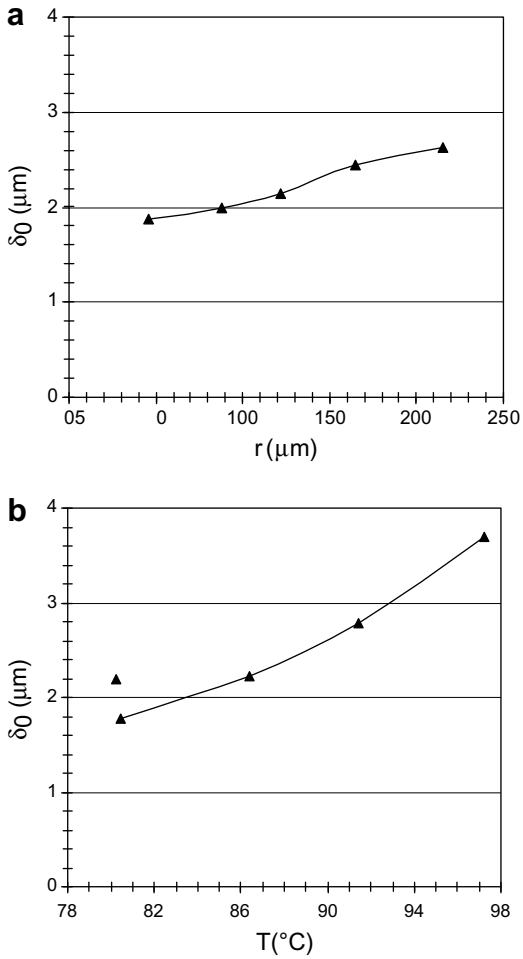

Fig. 7. Microlayer thickness (a) versus radius from the center of the bubble (at an average surface temperature of 86.4 °C) and (b) spatially-averaged (over maximum contact area) for different test conditions.

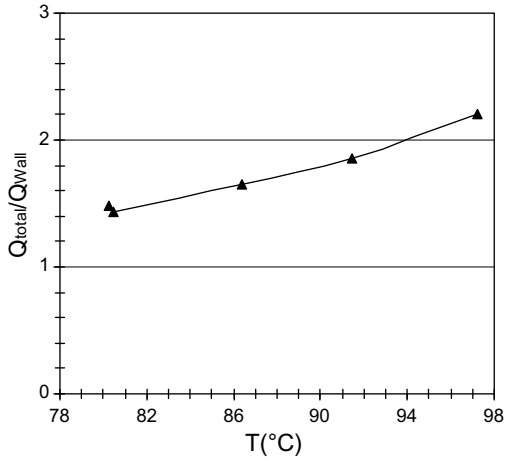

Fig. 8. Ratio of total microlayer evaporation energy and wall heat transfer.

1. As discussed earlier, Mikic and Rohsenow [7] (Eq. (11)) does not properly predict the transient conduction process. The current work indicated that this mode of heat transfer can be accurately modeled using the correlation derived in this study (Eq. (19)).
2. Our experimental results suggest that transient conduction heat flux is not active during the entire nucleation period. So, when different modes of heat transfer are added up, the activation period of this mechanism should be taken into account.
3. In all test conditions, it was found that the influence area of the transient conduction process is strictly limited to the contact area. Since the diameter of the contact area was found to be around $0.5D_b$, the activation area of the transient conduction process is therefore $0.25\pi R_b^2$ (i.e. $K = 0.25$).

The third term of the Judd and Hwang [12] correlation has also been separately compared with the convection heat transfer results outside the contact area (see Fig. 2). The fact that the natural convection model does not follow the trend observed in the experiment is more significant than the difference between the absolute values. This suggests that the natural convection model does not represent the physics of the heat transfer process in the region of interest. The results clearly suggest a convection effect triggered by the continuous departure of the bubbles, a net upward flow of liquid that is closely predicted by the Rohsenow [2] convection model.

5.2. Benjamin and Balakrishnan [13] model

Similar to the Judd and Hwang [12] analogy, Benjamin and Balakrishnan [13] assumed that microlayer evaporation, transient conduction, and natural convection heat transfer modes constitute the total surface heat flux. However, they made different assumptions concerning the activation time period and magnitude of these mechanisms. Their correlation is as follow:

$$q'' = \phi\pi R_b^2 n q''_{ME}\frac{t_g}{t_g+t_w} + 4\pi R_b^2 n q''_{TC}\frac{t_w}{t_g+t_w} + (1-4\pi R_b^2 n)q''_{NC} \qquad (27)$$

As can be seen in Eq. (27), Benjamin and Balakrishnan [13] assumed that the transient conduction mechanism is active over $4\pi R_b^2$ area. They also incorporated a factor to account for the activation period of different modes of heat transfer. They assumed that microlayer evaporation and transient conduction modes are active during the growth and waiting periods, respectively, and used Van Stralen et al. [22] who suggested the following relation between growth and waiting times (for pure liquids).

$$t_w = 3t_g \qquad (28)$$

Therefore, the time factors for microlayer evaporation term (1st term in Eq. (27)) and transient conduction term (2nd term in Eq. (27)) are 0.25 and 0.75, respectively. Benjamin and Balakrishnan [13] used Sernas and Hooper's [23] correlation for microlayer heat transfer to a growing bubble and Siegel and Keshock's [24] correlation for instantaneous diameter of the bubble to derive an expression for total microlayer volume. They divided the total evaporation energy of microlayer by t_g to determine q''_{ME}. To determine the transient conduction heat flux, they integrated the semi-infinite transient conduction correlation [18] over the waiting time,

$$q''_{TC} = 2\frac{k_l\Delta T}{\sqrt{\pi\alpha_l t_w}}, \qquad (29)$$

and used turbulent natural convection $Nu_{NC} = 0.14Ra^{1/3}$ to determine q''_{NC}.

The closure of Eq. (29) was then completed through use of Torikai et al. [25] results for $\phi(=(D_c/D_b)^2)$, Stephan's [26] correlation for D_b, and their own correlation for $n(=N/A_T)$. They found a close match between their correlation and experimental data on various surface and liquid combinations. Eventually, their model suggested that microlayer evaporation and transient conduction heat flux

together accounts for 90% of surface heat flux for water and 75–80% for organic fluids. Microlayer evaporation alone was suggested to be responsible for 50% of the total surface heat transfer for water and 45% for organic liquids.

Benjamin and Balakrishnan [13] have made a series of assumptions concerning different aspects of the heat transfer processes that do not apply to our experimental results. The differences are detailed as follow:

1. Our test results suggested that the transient conduction mechanism is only active over the contact area (approximately $0.25\pi R_b^2$) as oppose to $4\pi R_b^2$.
2. The activation time period of the microlayer evaporation mechanism is about half of t_g. Transient conduction heat transfer mainly takes place during the second half of t_g, when the contact line recedes and liquid rewets the contact area. This mode of heat transfer lasts for only a few milliseconds and diminishes on most of the surface before the bubble departure.
3. Benjamin and Balakrishnan [13] results suggested that wall heat transfer due to microlayer evaporation is greater than transient conduction. Since the ratio between the assumed activation areas of these two mechanisms is 16 ($4\pi R_b^2$ versus $0.25\pi R_b^2$), the magnitude of heat flux through microlayer evaporation should be more than 16 times greater than the transient conduction heat flux. The experimental results presented in part I of this study shows that heat flux through these mechanisms are in the same order.
4. As discussed in Section 4.1, surface rewetting during the transient conduction process is gradual. This factor should be taken into account when semi-infinite body transient conduction model [18] is adapted. An improved form of the transient conduction model for simulating heat transfer during the rewetting process is Eq. (19).
5. The natural convection correlation used by Benjamin and Balakrishnan [13] is similar to the one used by Judd and Hwang [12] with a slightly smaller constant coefficient (i.e. 0.14 versus 0.18). As discussed in the previous section, natural convection theory does not represent the physics of heat transfer observed outside the contact area.

6. Proposed model

In the previous sections, we analyzed/developed correlations that can accurately predict heat transfer through various mechanisms. In modeling the wall heat transfer through microlayer evaporation, the initial microlayer sensible energy is taken into account as follow

$$q''_{ME} = \rho_l(h_{fg} - C_l\Delta T)\bar{\delta}_0/t_m \tag{30}$$

Heat flux through transient conduction (q''_{TC}) and microconvection (q''_{MC}) mechanisms are determined using Eq. (19) and Rohsenow [2] model (Eq. (7) with $C_{sf} = 0.013$), respectively.

In order to combine heat transfer through different mechanisms, the activation time and influence area of different heat transfer mechanisms should be incorporated. Considering that microlayer and transient conduction mechanisms are active within and near the contact area and microconvection predominates outside this region, the following composite correlation is proposed as a logical evolution to previous models discussed above:

$$q'' = \phi\pi R_b^2 n\left(q''_{ME}\frac{t_m}{t_g + t_w} + q''_{TC}\frac{t_r}{t_g + t_w}\right) + (1 - \phi\pi R_b^2 n)q''_{MC} \tag{31}$$

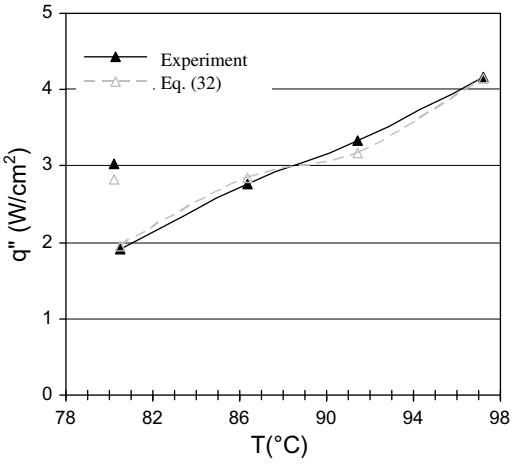

Fig. 9. Comparison between experimental surface heat flux and predicted by Eq. (32).

Knowing that $f = 1/(t_g + t_w)$ and $n = N/A_T = 1/\pi R_b^2$, Eq. (31) can be written in the following format.

$$q'' = \phi\left(\rho_l(h_{lv} - C_l\Delta T)\bar{\delta}_0 f + q''_{TC}t_r f\right) + (1 - \phi)q''_{MC} \tag{32}$$

The total surface heat flux was calculated using Eq. (32) at different surface temperatures (see Table 2 for different parameters). The results are compared with the experimental heat flux values in Fig. 9. As can be seen in the figure, results of Eq. (32) closely match the experimental values. This is not surprising in light of the fact that different mechanisms of heat flux were properly modeled in the previous sections. And, time period of activation and influence area of each mechanism were accurately factored into Eq. (32).

7. Closure

At this stage, we do not recommend using this model for fitting experimental data on large surfaces. As mentioned in the introduction section, bubble–bubble and bubble–liquid interactions result in secondary effects that need to be understood and then worked out into the developed model. We encourage more experimental and theoretical studies on these aspects over a wide parametric range. In our opinion, to build better boiling models, a bottom up approach should be taken to first develop a good understanding of the microscale physics of the nucleate boiling process and then sort out the existing models and develop new models based on the actual physics of the boiling processes. As we have shown in this study, combining unsubstantiated models and fitting them to integral experimental data often results in misrepresentation of the true nature of some of the boiling subprocesses. For example, one can readily fit a composite model to experimental data by varying parameters such as influence area of different mechanisms and their time period of activation and find wrong values for each parameter. Instead, efforts to relate these parameters to explicitly known boiling conditions (i.e. surface and liquid conditions) might be more fruitful.

8. Conclusions

The experimental results on FC-72 liquid in saturation conditions presented in the first part of this study were theoretically analyzed. The test data were compared with some of the typical boiling models. None of the existing models was found to accurately represent the actual physics of the heat transfer process observed in the tests. Deficiencies of the existing models as it relates to their fundamental assumptions were clearly identified. How-

ever, it was found that some of the models can predict the individual components of the surface heat transfer. The Rohsenow [2] model was found to accurately predict the microconvection portion of the surface heat transfer that is active outside the bubble/surface contact area and within the bubble projected area. Heat transfer in this region was not found to follow the natural convection theory.

Mikic and Rohsenow [7] transient conduction model was found to significantly overpredict the surface heat flux. A transient conduction model suggested by Demiray and Kim [19] was then modified to account for the gradual surface coverage by the liquid front during the rewetting process. When combined with incorporation of the consistent activation time, the new model was found to accurately predict the transient conduction heat flux.

Using the surface heat transfer during microlayer evaporation, the initial thickness and temperature of the microlayer was found. The initial temperature of the microlayer was found to be close to the heated wall temperature. Contribution of the microlayer initial sensible energy to the total energy required for its evaporation was found to be significant. It even exceeded the surface heat transfer at high surface superheat temperatures.

Through incorporation of the right models for the individual mechanisms of heat transfer, their activation time, and their influence area, a composite model was developed. The developed model closely matched the experimental heat transfer results.

References

[1] M. Jakob, W. Linke, Boiling heat transfer, Phys. Z. 636 (1935) 267–273.
[2] W.M. Rohsenow, A method of correlating heat transfer data for surface boiling of liquids, J. Heat Transfer 74 (1951) 969–976.
[3] C.L. Tien, Hydrodynamic model for nucleate pool boiling, Int. J. Heat Mass Transfer 5 (1962) 533–540.
[4] H. Schlichting, Boundary Layer Theory, McGraw-Hill, New York, 1960.
[5] N. Zuber, Nucleate boiling the region of isolated bubbles and the similarity with natural convection, Int. J. Heat Mass Transfer 6 (1962) 53–78.
[6] H.K. Forster, R. Greif, Heat transfer to a boiling liquid-mechanism and correlations, J. Heat Transfer 81 (1959) 43–54.
[7] B.B. Mikic, W.M. Rohsenow, A new correlation of pool boiling data including the effect of heating surface characteristics, J. Heat Transfer 91 (1969) 245–250.
[8] S.I. Haider, R.L. Webb, A transient micro-convection model of nucleate pool boiling, Int. J. Heat Mass Transfer 40 (1997) 3675–3688.
[9] C.J. Rallis, H.H. Jawurek, Latent heat transfer in saturated nucleate boiling, Int. J. Heat Mass Transfer 7 (1964) 1051–1068.
[10] C.Y. Han, P. Griffith, The mechanism of heat transfer in nucleate pool boiling-I and II, Int. J. Heat Mass Transfer 8 (1965) 887–914.
[11] R.W. Graham, R.C. Hendricks, Assessment of Convection and Evaporation in Nucleate Boiling, NASA TN D-3943 (1967).
[12] R.L. Judd, K.S. Hwang, A comprehensive model for nucleate pool boiling heat transfer including microlayer evaporation, J. Heat Transfer 98 (1976) 623–629.
[13] R.J. Benjamin, A.R. Balakrishnan, Nucleate pooling heat transfer of pure liquids at low to moderate heat fluxes, Int. J. Heat Mass Transfer 39 (1996) 2495–2504.
[14] P.C. Wayner, Y.K. LaCroix, The interline heat transfer coefficient of an evaporating wetting film, Int. J. Heat Mass Transfer 19 (1976) 487–492.
[15] V.K. Dhir, Boiling heat transfer, Annu. Rev. Fluid Mech. 30 (1998) 365–401.
[16] S. Moghaddam, K. Kiger, Physical mechanisms of heat transfer during nucleate boiling of FC-72 under saturation conditions-I. Experimental investigation, Int. J. Heat Mass Transfer (2008), doi:10.1016/j.ijheatmasstransfer.2008.08.018.
[17] H.K. Forster, N. Zuber, Dynamic of vapor bubbles and boiling heat transfer, AIChE J. 1 (1955) 531–539.
[18] H.S. Carslaw, J.C. Jaeger, Conduction of Heat in Solids, second ed., Oxford University Press, London, UK, 1959.
[19] F. Demiray, J. Kim, Microscale heat transfer measurements during pool boiling of FC-72: effect of subcooling, Int. J. Heat Mass Transfer 47 (2004) 3257–3268.
[20] C.M. Voutsinos, R.L. Judd, Laser interferometric investigation of the microlayer evaporation phenomenon, J. Heat Transfer 97 (1975) 88–92.
[21] S. Moghaddam, K. Kiger, A. Modafe, R. Ghodssi, A novel benzocyclobutene-based device for studying the dynamics of heat transfer during the nucleation process, J. MEMS 16 (2007) 1355–1366.
[22] S.J.D. Van Stralen, M.S. Sohal, R. Cole, W.M. Stuyter, Bubble growth rates in pure and binary systems: combined effect of relaxation and evaporation microlayers, Int. J. Heat Mass Transfer 18 (1975) 453–467.
[23] V. Sernas, F.C. Hooper, The initial vapor bubble growth on a heated wall during nucleate boiling, Int. J. Heat Mass Transfer 12 (1969) 1627–1639.
[24] R. Siegel, E.G. Keshock, Effects of reduced gravity on nucleate boiling bubble dynamics in water, AIChE J. 20 (1964) 509–517.
[25] K. Torikai, M. Hori, M. Akiyama, T. Kobori, H. Adachi, Boiling heat transfer and burn out mechanism in boiling water cooled reactor, Third United Nations International Conference on the Peaceful Uses of Atomic Energy (1964) (Paper No. 28/P/580).
[26] K. Stephan, Heat Transfer in Conduction and Boiling, Springer, New York, 1992.
[27] http://www.3M.com.